IEEE Photonics Journal
An IEEE Photonics Society Publication

Open Access

Highly Sensitive Temperature Sensor Based on Hollow Microsphere for Ocean Application

Volume 11, Number 6, December 2019

Gaofei Gu
Junfeng Jiang
Shuang Wang
Kun Liu
Yongning Zhang
Zhenyang Ding
Xuezhi Zhang
Tiegen Liu

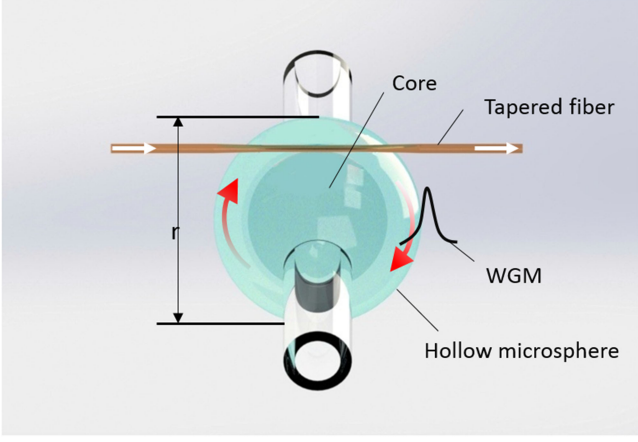

DOI: 10.1109/JPHOT.2019.2950028

IEEE photonics SOCIETY
IEEE

Highly Sensitive Temperature Sensor Based on Hollow Microsphere for Ocean Application

Gaofei Gu [1,2,3] Junfeng Jiang [1,2,3] Shuang Wang [1,2,3] Kun Liu [1,2,3] Yongning Zhang [1,2,3] Zhenyang Ding [1,2,3] Xuezhi Zhang [1,2,3] and Tiegen Liu [1,2,3]

[1]School of Precision Instrument and Opto-electronics Engineering, Tianjin University, Tianjin 300072, China
[2]Key Laboratory of Opto-electronics Information Technology, Ministry of Education, Tianjin University, Tianjin 300072, China
[3]Tianjin Optical Fiber Sensing Engineering Center, Institute of Optical Fiber Sensing, Tianjin University, Tianjin 300072, China

DOI:10.1109/JPHOT.2019.2950028

Manuscript received August 26, 2019; revised October 9, 2019; accepted October 24, 2019. Date of publication October 28, 2019; date of current version November 11, 2019. This work was supported in part by National Natural Science Foundation of China under Grants 61735011, 61675152, and 61505139, in part by Tianjin Natural Science Foundation under Grant 16JCQNJC02000, in part by National Instrumentation Program of China under Grant 2013YQ030915, in part by China Postdoctoral Science Foundation under Grant 2016M590200, in part by Tianjin Talent Development Special Plan for High Level Innovation and Entrepreneurship Team, and in part by the open project of Key Laboratory of Opto-electronics Information Technology under Grant 2019KFKT007. Corresponding authors: Junfeng Jiang, Shuang Wang, and Kun Liu (e-mail: jiangjfjxu@tju.edu.cn; shuangwang@tju.edu.cn; beiyangkl@tju.edu.cn).

Abstract: A highly sensitive temperature sensor based on hollow microsphere is demonstrated for ocean temperature measurements. The effect of sensor parameters on temperature sensitivity is investigated with the experiments using different parameters hollow microspheres, tapered fibers with different waist diameters and different kinds of solution. A high sensitivity of 396.70 pm/°C is obtained when the hollow microsphere is filled with ethanol. A high temperature resolution 1.75 $\times$ 10^{-3} °C is obtained when the hollow microsphere is filled with cyclohexane. The volatilization process of 2 μL ethanol is detected to demonstrate good dynamical response of the sensor.

Index Terms: Hollow microsphere, whispering gallery mode, temperature, ocean application.

1. Introduction

Temperature is an essential physical parameter of marine environment and needs to be acquired for studying the marine life, aquaculture, meteorological research, etc. Conductivity, Temperature and Depth (CTD) profiler [1] based on electric sensor has widely been used in ocean application. Recently, CTD profilers based on optical fiber sensors attract intensive attention since optical fiber sensors are electrical passive and less vulnerable to the water penetration induced short-circuit damage. Many optical fiber temperature sensors based on fiber Bragg grating, Fabry-Perot and photonic crystal fiber has been proposed. Though the measurement range of temperature sensor for ocean is only from -5 °C to 35 °C, the high temperature resolution ($\sim$0.0002 °C to 0.01 °C)

is required. Thus highly sensitive optical temperature sensor is needed. Microresonator with high quality factor (Q-factor) can excite and sustain whispering gallery mode (WGM), so it is a highly sensitive optical structure. WGM microresonators with various geometries, such as microdisks [2], [3], microtoroids [4], [5], microrings [6], [7], microspheres [8], [9] have been proposed for bio-sensing [10], [11], refractive index sensing [12], [13], pressure sensing [14], [15], magnetic field sensing [16], [17] and so on. Some researches focus on temperature sensing using microsphere sensors. Yan *et al*. [18] prepared a packaged silica microsphere by melting the end of the fiber. A sensitivity of 13.37 pm/°C is obtained, and the resolution is 1.1×10^{-3} °C. Although the silica microsphere sensor has high temperature resolution, its low sensitivity leads to a requirement of high-resolution spectrometer (∼0.015 pm). Dong *et al*. [19] used a microsphere with polydimethylsiloxane (PDMS) material as the temperature sensor. The sensitivity is 245 pm/°C, and the resolution is 2.0×10^{-4} °C when temperature changes from 22 °C to 32 °C. The structure is relatively fragile because PDMS microsphere is stuck to the suspended taper fiber stem. In addition to solid state microspheres, liquid microspheres are also used to sense the temperature, such as nematic liquid crystal droplet [20], 2-[2-[4-(dimethylamino)phenyl]ethenyl]-6-methyl-4H-pyran-4-ylidene doped oil droplet [21], dye-doped cholesteric liquid crystal droplet [22], etc. The liquid microspheres have relatively higher sensitivity (∼267 pm/°C to 1500 pm/°C). But they are easily affected by environment and evaporating, which prevent them from long-term measurement or reutilization. Microbubble sensors are also used for temperature measurement. He *et al*. [23] used polymethylmethacrylate to fabricate microbubble, but the sensitivity of 39 pm/°C is relatively low. Ward *et al*. [24] heated silica glass capillary with CO_2 laser to form microbubble. The microbubble was filled with ethanol, and the sensitivity of 200 pm/°C and resolution of 8.5×10^{-3} °C were realized when temperature rose from 23.95 °C to 24.95 °C. Different from conventional solid core microspheres, hollow microspheres or microbubbles can be flexibly adjusted with more parameters. Apart from temperature sensing, the thin walls of hollow microspheres make them more sensitive to pressure changes and have a nature fluidic channel for salinity sensing, which make them a good sensing element for compact ocean all-optical CTD profile.

In this paper, we construct a highly sensitive temperature sensor based on hollow microsphere for ocean temperature measurements. Hollow microspheres with different parameters, tapered fibers with different waist diameters and different kinds of solution have been introduced to investigate their effects on temperature sensing. The sensors filled with ethanol are measured from 0 °C to 36 °C, which covers the main temperature range (2 °C to 30 °C) in ocean application. A high sensitivity of 396.70 pm/°C is obtained when the hollow microsphere is filled with ethanol. A hollow microsphere sensor is filled with ethanol, acetone and cyclohexane in sequence when temperature changes from 25 °C to 26 °C. A high temperature resolution 1.75×10^{-3} °C is obtained when the hollow microsphere is filled with cyclohexane. The volatilization process of 2 μL ethanol has been detected to demonstrate good dynamical response of the sensor.

2. Principle

Fig. 1(a) shows the schematic diagram of the temperature sensor. The sensor is consist of a hollow microsphere, injected solution and a tapered fiber. WGM resonance conditions can be expressed as: $2\pi n_{eff} r = m\lambda_{a,l,q}$, where r is the outer radius of the hollow microsphere, $\lambda_{a,l,q}$ is the WGM resonant wavelength, a, l and q are the angular mode number, the radial mode number and axial mode number, respectively. And n_{eff} is the corresponding effective refractive index. Temperature-induced wavelength shift variation is related to the material thermal expansion effect and the effective refractive index change, and the effective refractive index change rate can be expressed as follows [25]:

$$\frac{\partial n_{eff}}{\partial T} = k_{air}\frac{\partial n_{eff}}{\partial n_{air}} + k_{core}\frac{\partial n_{eff}}{\partial n_{core}} + k_{wall}\frac{\partial n_{eff}}{\partial n_{wall}} + \alpha_{wall}\frac{\partial n_{eff}}{\partial t}, \tag{1}$$

where n_{air}, n_{core} and n_{wall} are the refractive indices of the air outside the hollow microsphere, the core and the glass, respectively. k_{air}, k_{core} and k_{wall} are the corresponding thermo-optic coefficients.

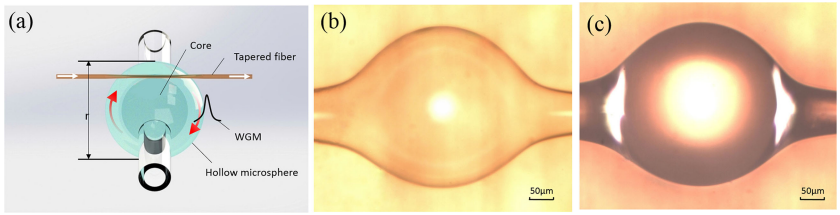

Fig. 1. (a) Schematic diagram of the temperature sensor. (b) The microscopic picture of the hollow microsphere with outer diameter 350.4 μm. (c) The microscopic picture of the same hollow microsphere filled with ethanol.

α_{wall} is the thermal expansion coefficient of the glass. t is the wall thickness. k_{air} and α_{wall} are relatively small, so the terms $k_{air}(\partial n_{eff}/\partial n_{air})$ and $\alpha_{wall}(\partial n_{eff}/\partial t)$ can be ignored. Finally, the resonance wavelength temperature response or sensitivity can be expressed as:

$$S_T = d\lambda/dT = \lambda\left(\alpha + \frac{k_{core}}{n_{eff}}\frac{\partial n_{eff}}{\partial n_{core}} + \frac{k_{wall}}{n_{eff}}\frac{\partial n_{eff}}{\partial n_{wall}}\right), \tag{2}$$

where $\alpha = 5 \times 10^{-7}{}^{\circ}\mathrm{C}^{-1}$, $k_{wall} = 11 \times 10^{-7}{}^{\circ}\mathrm{C}^{-1}$, $n_{wall} = 1.45$ for silica material, k_{core} and n_{core} are determined by the solution injected. Take ethanol as an example, $k^e_{core} = -3.9 \times 10^{-4}{}^{\circ}\mathrm{C}^{-1}$, $n^e_{core} = 1.365$. The wall has a positive thermo-optic coefficient and a positive thermal expansion coefficient. However, the ethanol has a negative thermo-optic coefficient. The joint action of three factors will make the resonance wavelength produce blue shift, i.e., resonance wavelength shifts to short wavelength band. Assuming that the light field is 90%∼95% lies in the ethanol core, which can be adjusted by the wall thickness and the outer diameter of the hollow microsphere, the theoretical temperature sensitivity can be 390.77 pm/°C∼414.51 pm/°Cusing Eq. (2).

The temperature resolution of the hollow microsphere sensor can be calculated as: $\Delta T_{rso} = \Delta\lambda_{\min}/S_T$, where $\Delta\lambda_{\min}$ is spectral resolution, which is about one hundredth of the full width half maximum of the spectral line [26].

3. Sensor Fabrication

The fabrication of the hollow microsphere has been reported in Ref. 27. Hollow microspheres are made by two steps. In the first step, a silica capillary (TSP250350, Polymicro Inc.) is stretched under the hydrogen oxide flame. At the same time, air with a set pressure is pumped into the capillary to decrease the wall thickness and avoid capillary collapse. In the second step, thin wall silica capillary is locally heated by another smaller hydrogen oxide flame nozzle while keep air pressure inside capillary unchanged. Thus, the silica capillary swells and takes shape into a smooth sphere by surface tension. In order to protect the hollow microsphere, it is fixed on a copper sheet by epoxy glue. Hollow microspheres with different outer diameters and wall thicknesses can be fabricated by adjusting the flame size, the stretching length and the internal air pressure. Based on the method above, hollow microspheres with outer diameters ranging from 300 μm to 500 μm are fabricated. A hollow microsphere with 350.4 μm diameter is shown in Fig. 1(b). The hollow microsphere can be filled with different solutions. Fig. 1(c) shows the microscope image of the same hollow microsphere filled with ethanol. Tapered fibers used for WGM excitation are also fabricated by the flame-heated stretching technique. The internal pressure can lead to the change of effective refractive index and hollow microsphere size, thus the resonance wavelength is shifted. Based on this, the wall thickness is deduced by the following formula [28]:

$$t = r \cdot \left[1 - \left(\frac{S_P}{A + S_P}\right)^{1/3}\right], \tag{3}$$

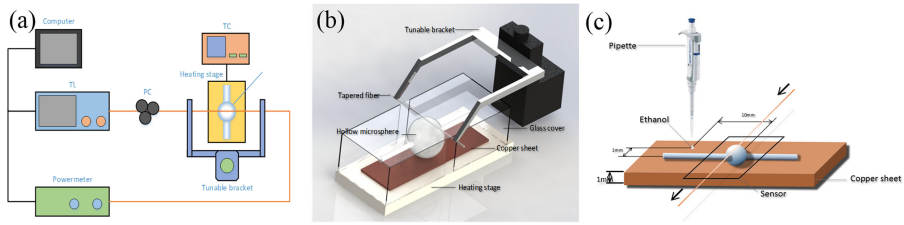

Fig. 2. (a) Schematic diagram of the temperature sensing measurements. (b) 3D layout of the hollow microsphere coupled to the tapered fiber. TL: tunable laser, PC: polarization controller, TC: temperature controller. (c) The local experimental diagram of monitoring the temperature of ethanol volatilization process.

TABLE 1
Parameters of Five Sensors

Number	Outer diameter	Measured thickness	Q-factor (ethanol core)	Temperature sensitivity	Temperature resolution
#1	444.0 μm	1.834 μm	2.34×10^3	396.7 0pm/°C	1.67×10^{-2}° C
#2	374.4 μm	1.074 μm	2.27×10^3	315.6 5pm/°C	2.15×10^{-2}° C
#3	350.4 μm	1.905 μm	5.14×10^3	202.9 8pm/°C	1.48×10^{-2}° C
#4	456.0 μm	3.865 μm	3.08×10^3	126.3 9pm/°C	3.96×10^{-2}° C
#5	367.2 μm	2.683 μm	2.67×10^3	92.90 pm/°C	6.24×10^{-2}° C

where t is the wall thickness, S_P is the pressure sensitivity, A is a constant related to the refractive index of the hollow microsphere, elastic-optic constant and the shear and bulk moduli of the silica.

4. Experimental Setup

Fig. 2(a) illustrates the temperature sensing experimental setup of the hollow microsphere sensor. The light, output from a tunable laser (Keysight 81607A, linewidth $<$10 kHz), passes through a polarization controller for polarization adjustment, and then it is coupled into the hollow microsphere through a tapered fiber. The transmitted light from tapered fiber is detected by an optical powermeter (Keysight 81636B). The WGM spectrum is acquired by sweeping the center wavelength of light source. The sensor is placed on a heating station with high precision temperature controller. A glass cover is placed above the sensor in order to avoid external factors affecting the measurement. Fig. 2(b) shows the 3D layout of the hollow microsphere coupled to the tapered fiber.

Five hollow microspheres with outer diameters 350.4 μm, 367.2 μm, 374.4 μm, 456.0 μm and 444.0 μm are used for experiment. They are all filled with ethanol. The waist diameter of tapered fiber is 2.7 μm. A detail information of these five sensors is presented in Table 1. Fig. 3 shows the resonant wavelength variation of the transmission spectrum of the #1 sensor within 1 °C temperature change. It can be seen that the resonance wavelength makes a blue shift as theoretical expectation.

The proposed sensors are then used to measure the temperature from 0 °C to 36 °C stepped by 2 °C, which covers the main temperature range (2 °C$\sim$30 °C) in ocean application. The dwell time at each temperature is 30 s to ensure that the temperature is stable during the data acquisition. Fig. 4(a) shows the relationship between the resonance wavelength shift $\Delta\lambda$ and the temperature change ΔT. The temperature sensitivities of five sensors are in the range of 92.90 pm/°C to 396.70 pm/°C. By comparing #2 sensor and #3 sensor, it can be seen that these two hollow microspheres' outer diameters are close and the sensor with thin wall realizes a relatively high sensitivity. For hollow microspheres with same outer diameters, the light field in the ethanol core is higher when the glass wall is thinner. Thus a higher temperature sensitivity is achieved. At

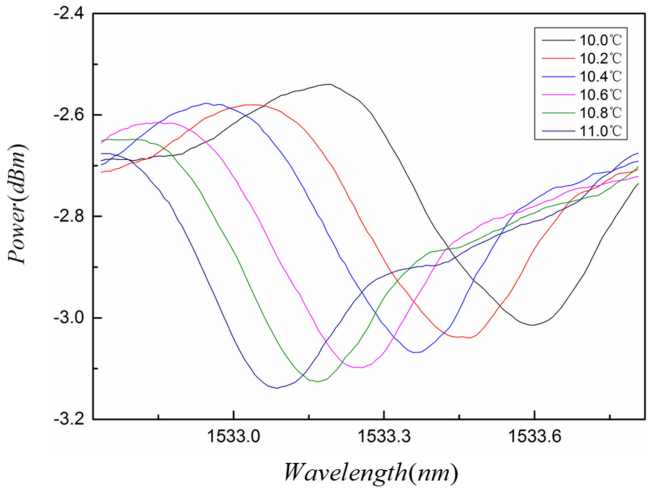

Fig. 3. Transmission spectrum of the sensor from 10 to 11, with the increase of temperature, the spectrum experiences a blue shift.

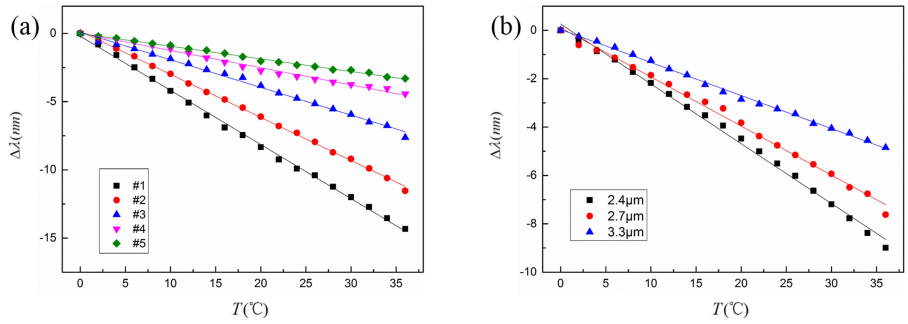

Fig. 4. (a) Resonant wavelength shift of five different sensors versus temperature. (b) The measured temperature sensitivities of the #3 hollow microsphere coupled with three different fiber tapers. The solid lines are the linear fitting results.

the same time, by comparing #1 sensor and #3 sensor, it can be seen that the wall thickness of these two hollow microspheres are close. The larger the outer diameter is, the higher the temperature sensitivity is. This is because that, when the wall thickness is the same and the outer diameter is large, the ratio of the wall thickness to the outer diameter is small and the light field in the ethanol is also high. Since the temperature resolution of #3 hollow microsphere is the highest and the outer diameter of it is the smallest among the five hollow microspheres, this hollow microsphere is selected for further experiment. In addition, the influences of tapered fibers with different waist diameters have also been investigated and the result is presented in Fig. 4(b). Waist diameters of three tapered fibers are 2.4 μm, 2.7 μm and 3.3 μm, corresponding the temperature sensitivities are 247.23 pm/°C, 202.98 pm/°C and 136.62 pm/°C, respectively. For a microsphere with a fixed size, the tapered fiber with smaller waist diameter can couple to higher radial modes [29]. The higher the number of radial mode, the higher the light field distribution in the ethanol core, thus the temperature sensitivity is also increased.

In addition, unlike conventional microspheres, the temperature sensitivity of hollow microspheres can be changed by filling different solutions. The higher the absolute value of the thermo-optic coefficient of the internal solution, the higher the sensitivity of the temperature sensing. Three solutions (ethanol, acetone, cyclohexane) are injected into the #3 hollow microsphere for temperature sensing experiments. The thermo-optic coefficients of ethanol, acetone and cyclohexane

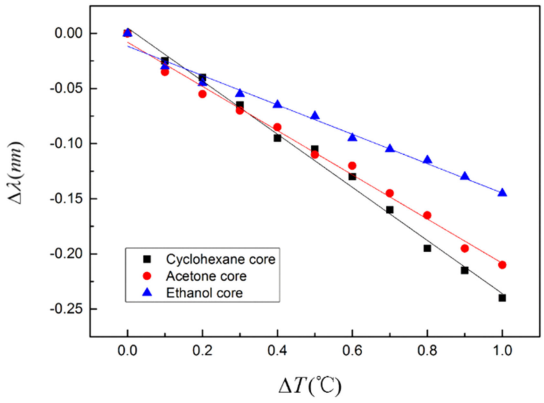

Fig. 5. The measured temperature sensitivities of the #3 hollow microsphere with three different solutions injected. The solid lines are the linear fitting results.

TABLE 2
Comparisons of Different Optical Fiber Sensors Developed for Ocean Temperature Sensing

Sensor structure	Temperature sensitivity	Advantage	Disadvantage	Published year
Three-wave fiber Fabry–Perot [30]	29 pm/°C	Simultaneous measurement of temperature and salinity	Low temperature sensitivity	2011
Microfiber knot resonator [31]	22.81 pm/°C	Small size	Low temperature sensitivity, fragile	2014
High-birefringence elliptic fiber Sagnac loop [32]	472 pm/°C	High temperature sensitivity	Bulky size	2015
Fibre Bragg Gratings [33]	12.5 pm/°C	Good stability	Low temperature sensitivity	2017
Hollow microsphere filled with ethanol (this paper)	396.70 pm/°C	High temperature sensitivity, small size	Fragile	\

are $k^e_{core} = -3.9 \times 10^{-4}\,^{\circ}\mathrm{C}^{-1}$, $k^a_{core} = -5.0 \times 10^{-4}\,^{\circ}\mathrm{C}^{-1}$, $k^c_{core} = -5.4 \times 10^{-4}\,^{\circ}\mathrm{C}^{-1}$, respectively. The deionized water is used to rinse the hollow microsphere for 5 min at first when different solutions are injected. The temperature in experiment increases from 25 °C to 26 °C with a step of 0.1 °C, and the results are shown in Fig. 5. The temperature sensitivities of ethanol, acetone and cyclohexane are 133.18 pm/°C, 200.45 pm/°C and 240.91 pm/°C, respectively. The experimental results are consistent with the theoretical analysis. The Q-factor of the hollow microsphere filled with cyclohexane is estimated to be 3.85×10^4, and the corresponding temperature resolution is 1.75×10^{-3} °C.

A detail information about previous different optical fiber sensors developed for ocean temperature sensing is presented in Table 2. From Table 2, we can see that the hollow microsphere sensor in this paper has the advantages of small size and high temperature sensitivity.

The volatilization of ethanol is introduced to demonstrate the dynamical response of our sensors. The volatilization of ethanol absorbs heat and will result in a dynamical temperature variation. The experimental setup is shown in Fig. 2(c). The 2 μL ethanol droplet (99.8% volume concentration) is dropped on the copper sheet, which is used to fix the hollow microsphere, at room temperature. It repeats three times. Fig. 6 shows the dynamical response of the sensor. The temperature decreases rapidly at first and then increases slowly. The drop of the temperature means that ethanol

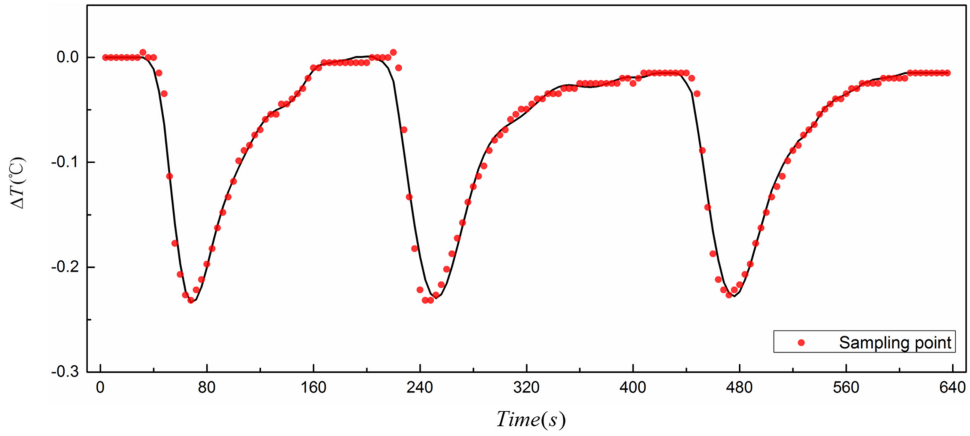

Fig. 6. The temperature variation during the 2 μL ethanol volatilization process. The solid line is the fitting result.

volatilization absorbs heat from the copper sheet. Then because the temperature of surrounding is higher than that of the copper sheet, the temperature rises to a steady value. It takes about 22 s for 2 μL ethanol to be completely volatilized, calculated by the temperature dropping from 10% to 90% of the steady value. The total temperature change during the volatilization of ethanol is around 0.23 °C.

5. Conclusion

In conclusion, we have studied hollow microspheres for temperature sensing from 0 °C to 36 °C. At the same time, the effect of the parameters including hollow microspheres, the waist diameters of tapered fibers and different kinds of solution on the temperature sensitivity have also been investigated. A high temperature sensitivity of 396.70 pm/°C is realized when the hollow microsphere is filled with ethanol. A high temperature resolution 1.75 $\times$ 10^{-3} °C is obtained when the hollow microsphere is filled with cyclohexane. The temperature dynamical trace of ethanol volatilization process is detected with the proposed temperature sensor, which demonstrates good dynamical response of the sensor. High sensitivity, high resolution, small size and simple fabrication process make the hollow microsphere sensor a promising candidate for ocean temperature sensing. Subsequently, package the sensor is needed. One possible approach is using the ultraviolet polymer to package the coupling part of the sensor, and the whole system can be solidified in a metal cover, which can prevent water intrusion and avoid the environmental pressure affecting the performance of the sensor.

References

[1] D. L. Rudnick and J. Klinke, "The underway conductivity-temperature-depth instrument," *J. Atmospheric Ocean. Technol.*, vol. 24, no. 11, pp. 1910–1923, 2007.
[2] E. Krioukov, D. J. W. Klunder, A. Driessen, J. Greve, and C. Otto, "Sensor based on an integrated optical microcavity," *Opt. Lett.*, vol. 27, no. 7, pp. 512–514, 2002.
[3] T. Ma *et al.*, "Simultaneous measurement of the refractive index and temperature based on microdisk resonator with two whispering-gallery modes," *IEEE Photon. J.*, vol. 9, no. 1, Feb. 2017, Art. no. 6800913.
[4] D. K. Armani, T. J. Kippenberg, S. M. Spillane, and K. J. Vahala, "Ultra-high-Q toroid microcavity on a chip," *Nature*, vol. 421, pp. 925–928, 2003.
[5] L. Xu *et al.*, "High-Q silk fibroin whispering gallery microresonator," *Opt. Exp.*, vol. 24, no. 18, pp. 20825–20830, 2016.
[6] A. L. Washburn, L. C. Gunn, and R. C. Bailey, "Label-free quantitation of a cancer biomarker in complex media using silicon photonic microring resonators," *Analytical Chem.*, vol. 81, no. 22, pp. 9499–9506, 2009.
[7] C. Wang *et al.*, "Highly sensitive optical temperature sensor based on a SiN micro-ring resonator with liquid crystal cladding," *Opt. Exp.*, vol. 24, no. 2, pp. 1002–1007, 2016.

[8] F. Vollmer, D. Braun, A. Libchaber, M. Khoshsima, I. Teraoka, and S. Arnold, "Protein detection by optical shift of a resonant microcavity," *Appl. Phys. Lett.*, vol. 80, no. 21, pp. 4057–4059, 2002.
[9] G. C. Righini and S. Soria, "Biosensing by WGM microspherical resonators," *Sensors*, vol. 16, 2016, Art. no. 905.
[10] Y. Wu, D. Zhang, P. Yin, and F. Vollmer, "Ultraspecific and highly sensitive nucleic acid detection by integrating a DNA catalytic network with a label-free microcavity," *Small*, vol. 10, no. 10, pp. 2067–2076, 2014.
[11] H. Ghali, P. Bianucci, and Y. Peter, "Wavelength shift in a whispering gallery microdisk due to bacterial sensing: A theoretical approach," *Sens. Bio-Sensing Res.*, vol. 13, pp. 9–16, 2017.
[12] Y. Kang, A. François, N. Riesen, and T. M. Monro, "Mode-splitting for refractive index sensing in fluorescent whispering gallery mode microspheres with broken symmetry," *Sensors*, vol. 18, 2018, Art. no. 2987.
[13] F. Sedlmeir, R. Zeltner, G. Leuchs, and H. G. L. Schwefel, "High-Q MgF2 whispering gallery mode resonators for refractometric sensing in aqueous environment," *Opt. Exp.*, vol. 22, no. 25, pp. 30934–30942, 2014.
[14] Y. Yang, S. Saurabh, J. Ward, and S. N. Chormaic, "Coupled-mode-induced transparency in aerostatically tuned microbubble whispering-gallery resonators," *Opt. Lett.*, vol. 40, no. 8, pp. 1834–1837, 2015.
[15] A. Bianchetti, A. Federicoa, S. Vincent, S. Subramanianb, and F. Vollmer, "Refractometry-based air pressure sensing using glass microspheres as high-Q whispering-gallery mode microresonators," *Opt. Commun.*, vol. 394, pp. 152–156, 2017.
[16] E. Freeman, C. Wang, V. Sumaria, S. J. Schiff, Z. Liu, and S. Tadigadapa, "Chip-scale high Q-factor glassblown microspherical shells for magnetic sensing," *AIP Advances*, vol. 8, no. 6, 2018, Art. no. 065214.
[17] A. Mahmood *et al.*, "Magnetic field sensing using whispering-gallery modes in a cylindrical microresonator infiltrated with ferronematic liquid crystal," *Opt. Exp.*, vol. 25, no. 11, pp. 12195–12202, 2017.
[18] Y. Yan *et al.*, "Packaged silica microsphere-taper coupling system for robust thermal sensing application," *Opt. Exp.*, vol. 19, no. 7, pp. 5753–5759, 2011.
[19] C. Dong *et al.*, "Fabrication of high-polydimethylsiloxane optical microspheres for thermal sensing," *Appl. Phys. Lett.*, vol. 94, no. 23, 2009, Art. no. 231119.
[20] Y. Wang, H. Li, L. Zhao, Y. Liu, S. Liu, and J. Yang, "Tapered optical fiber waveguide coupling to whispering gallery modes of liquid crystal microdroplet for thermal sensing application," *Opt. Exp.*, vol. 25, no. 2, pp. 918–926, 2017.
[21] Z. Liu *et al.*, "Whispering gallery mode temperature sensor of liquid microresonastor," *Opt. Lett.*, vol. 41, no. 20, pp. 4649–4652, 2016.
[22] Y. Wang, H. Li, L. Zhao, Y. Liu, S. Liu, and J. Yang, "Tunable whispering gallery modes lasing in dye-doped cholesteric liquid crystal microdroplets," *Appl. Phys. Lett.*, vol. 109, no. 23, 2016, Art. no. 231906.
[23] C. He *et al.*, "Temperature sensor based on high-Q polymethylmethacrylate optical microbubble," *Laser Phys.*, vol. 28, 2018, Art. no. 076202.
[24] J. M. Ward, Y. Yang, and S. N. Chormaic, "Highly sensitive temperature measurements with liquid-core microbubble resonators," *IEEE Photon. Technol. Lett.*, vol. 25, no. 23, pp. 2350–2353, Dec. 2013.
[25] J. D. Suter, I. M. White, H. Zhu, and X. Fan, "Thermal characterization of liquid core optical ring resonator sensors," *Appl. Opt.*, vol. 46, no. 3, pp. 389–396, 2007.
[26] F. Vollmer and S. Arnold, "Whispering-gallery-mode biosensing: Label-free detection down to single molecules," *Nature Methods*, vol. 5, no. 7, pp. 591–596, 2008.
[27] Z. Yu *et al.*, "High Q silica microbubble resonators fabricated by heating a pressurized glass capillary," *Proc. SPIE*, vol. 9274, 2014, Art. no. 92740L.
[28] Q. Lu, J. Liao, S. Liu, X. Wu, L. Liu, and L. Xu, "Precise measurement of micro bubble resonator thickness by internal aerostatic pressure sensing," *Opt. Exp.*, vol. 24, no. 18, pp. 20855–20861, 2016.
[29] J. C. Knight, G. Cheung, F. Jacques, and T. A. Birks, "Phase-matched excitation of whispering-gallery-mode resonances by a fiber taper," *Opt. Lett.*, vol. 22, no. 15, pp. 1129–1131, 1997.
[30] L. V. Nguyen, M. Vasiliev, and K. Alameh, "Three-wave fiber Fabry–Pérot interferometer for simultaneous measurement of temperature and water salinity of seawater," *IEEE Photon. Technol. Lett.*, vol. 23, no. 7, pp. 450–452, Apr. 2011.
[31] H. Yang, S. Wang, X. Wang, Y. Liao, and J. Wang, "Temperature sensing in seawater based on microfiber knot resonator," *Sensors*, vol. 14, pp. 18515–18525, 2014.
[32] X. Wang, H. Yang, S. Wang, Y. Liao, and J. Wang, "Seawater temperature measurement based on a high-birefringence elliptic fiber Sagnac loop," *IEEE Photon. Technol. Lett.*, vol. 27, no. 16, pp. 1772–1775, Aug. 2015.
[33] D. B. Duraibabu, G. Leen, D. Toal, T. Newe, E. Lewis, and G. Dooly, "Underwater depth and temperature sensing based on fiber optic technology for marine and fresh water applications," *Sensors*, vol. 17, 2017, Art. no. 1228.